Front. Electr. Electron. Eng. China 2008, 3(2): 176–182
DOI 10.1007/s11460-008-0031-5

RESEARCH ARTICLE

Jianxiong ZHOU, Zhiguang SHI, Qiang FU

A novel scheme for global scattering center modeling of radar targets

Abstract A novel scheme for extracting the global scattering center model of radar targets is proposed in this paper. The 2D/3D scattering center models can be reconstructed based on the wideband measurements at different viewing angles. The sphere spreading of the 1D scattering center projections is exploited. The 1D–2D/3D scatterer map (OTSM) is designed to manifest the high dimensional scattering characteristic of radar targets. The Hough transform and the least squares method are used to extract the stable scattering centers and their scattering coefficients. This modeling method does not need a high density of the spatial grid, which greatly cuts down the necessary original data. The model built in this way describes the stable point scattering mechanisms in a large spatial extent and can be extrapolated to other frequencies in the optical region. Examples verify the validity of both the model and the method.

Keywords radar target, scattering center, global, signature reconstruction

1 Introduction

The radar response of a target at high frequencies can be well approximated as coming from a few point scatterers, i.e., scattering centers. The scattering center model provides a concise and physically relevant description of radar targets, and is especially useful in radar data compression, signature prediction and target recognition. Modeling radar targets as scattering centers is always pursued by radar researchers. There are two ways for scattering center modeling. One is decomposing the target into several simple components, and obtaining the scattering center model by analyzing the scattering characteristics of each component [1,2]. This is quite subjective and therefore it is difficult to realize automatically. Another is extracting the position, amplitude, frequency and aspect characteristic of scattering centers from the wideband measurements or electromagnetic simulation data. It is in fact a parameter estimation problem and a research hotspot since the 1990s [3–7]. The problem in this modeling method is that it only represents the target characteristics in a small angular extent, i.e., the model is a local model [3–5]. R. Bhalla et al. proposed a method to extract the global scattering center model of a complex target by establishing correspondence among the local scattering centers extracted at various aspect angles [6,7]. However, since the global model is extracted from 3D images at different aspect angles which cover the angular extent of interest in a mesh style, the original data amount would have been very extensive had it not been for the one-look ISAR ability of the shooting and bouncing ray (SBR) technique to achieve the 3D images. Therefore, this method seems to be infeasible with measured data or data predicted by other high frequency electromagnetic simulation code, where the 3D imaging needs a synchronized azimuth-multiplying-elevation aperture with a very large data amount.

Here we propose another method to extract the global model from multiple 1D radar images, i.e., high range resolution profiles. It exploits the sphere placement of the projection points of a stable scattering center to establish the correspondence among the range profiles at different viewing angles, and estimates the scattering coefficient matrix of each scattering center by least squares method. The extracted scattering center model is a global one and can be used to reconstruct the target signatures, such as RCS data and radar images at any viewing angle in the angular extent covered by the original data and at any frequencies in or near the band of the original data. The extraction method does not need the synchronized aperture for 3D imaging, so it greatly cuts down the data amount necessary for global modeling. Moreover, the intermediate data form we devise, OTSM, shows the variation in the scattering center's amplitude and position with the change of the viewing

Translated from *Chinese Journal of Radio Science*, 2007, 22(3): 436–441 [译自: 电波科学学报]

Jianxiong ZHOU (✉), Zhiguang SHI, Qiang FU
ATR Loboratory, School of Electronics Science and Engineering, National University of Defense Technology, Changsha 410073, China
E-mail: zjxjanet@yahoo.com.cn

angle directly. Also, it is a useful tool to analyze the target scattering characteristics.

2 Basic principles

The spatial relation between radar and target is shown in Fig. 1. The coordinate system is bound on the target, and the line-of-sight (LOS) of the radar can be represented by azimuth angle θ and elevation angle γ. The target response at frequency f and viewing angle (θ, γ) can be predicted by the geometric theory of diffraction (GTD) based scattering center model as follows [8]:

$$E(\theta, \gamma, f) = \sum_{m=1}^{M} A_m(\theta, \gamma) \left(\frac{f}{f_0}\right)^{a_m} \mathrm{e}^{-\mathrm{j}4\pi f(x_m \cos\gamma\cos\theta + y_m \cos\gamma\sin\theta + z_m \sin\gamma)/\mathrm{c}}, \quad (1)$$

where E is the overall scattering field at frequency f. The time modulation factor $\exp(\mathrm{j}2\pi ft)$ is omitted, M is the scattering center number, (x_m, y_m, z_m), A_m, α_m denote the spatial location, scattering coefficient and type parameter of the mth scattering center, respectively. These parameters can be estimated from the measurement of $E(\theta, \gamma, f)$.

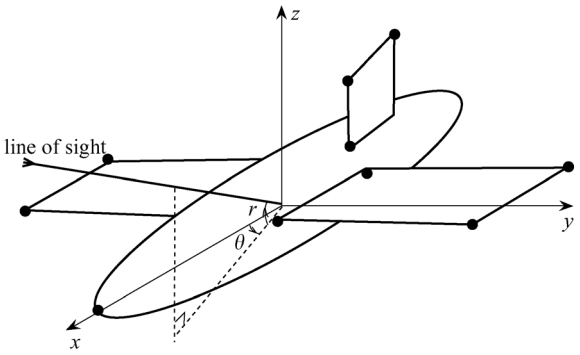

Fig. 1 Spatial relation between radar and target

The 1D projective position of each scattering center can be estimated from the wideband measurements at this viewing angle:

$$r_m(\theta, \gamma) = x_m \cos\gamma\cos\theta + y_m \cos\gamma\sin\theta + z_m \sin\gamma. \quad (2)$$

We always display the 1D projection of the 1D scattering center model by range profiles but this profile leaves out the information of the viewing angle. If we put each projection point on the line of sight, then the coordinate of this point in the Cartesian coordinates system should be:

$$\begin{aligned} x_P &= r_m \cos\gamma\cos\theta \\ &= x_m \cos^2\gamma\cos^2\theta + y_m \cos^2\gamma\sin\theta\cos\theta \\ &\quad + z_m \sin\gamma\cos\gamma\cos\theta, \end{aligned} \quad (3a)$$

$$\begin{aligned} y_P &= r_m \cos\gamma\sin\theta \\ &= x_m \cos^2\gamma\sin\theta\cos\theta + y_m \cos^2\gamma\sin^2\theta \\ &\quad + z_m \sin\gamma\cos\gamma\sin\theta, \end{aligned} \quad (3b)$$

$$\begin{aligned} z_P &= r_m \sin\gamma \\ &= x_m \sin\gamma\cos\gamma\cos\theta + y_m \sin\gamma\cos\gamma\sin\theta \\ &\quad + z_m \sin^2\gamma. \end{aligned} \quad (3c)$$

It is easy to prove that at any viewing angle, the coordinates satisfy

$$\left(x_P - \frac{x_m}{2}\right)^2 + \left(y_P - \frac{y_m}{2}\right)^2 + \left(z_P - \frac{z_m}{2}\right)^2 = \frac{1}{4}\left(x_m^2 + y_m^2 + z_m^2\right). \quad (4)$$

Equation (4) shows that the projection points of a fixed scattering center (i.e., its location (x_m,y_m,z_m) is independent of viewing angles) are always on a sphere with center $(x_m/2,y_m/2,z_m/2)$ and radius $\sqrt{x_m^2+y_m^2+z_m^2}/2$. This rule can be easily explained geometrically as shown in Fig. 2 for a 2D case. The scattering center, the system origin and the projection point form a right triangle and the projection point is the right angle vertex. The right angle vertexes of all the right triangles that share the same bevel edge will form a sphere, so do the projection points of a fixed scattering center.

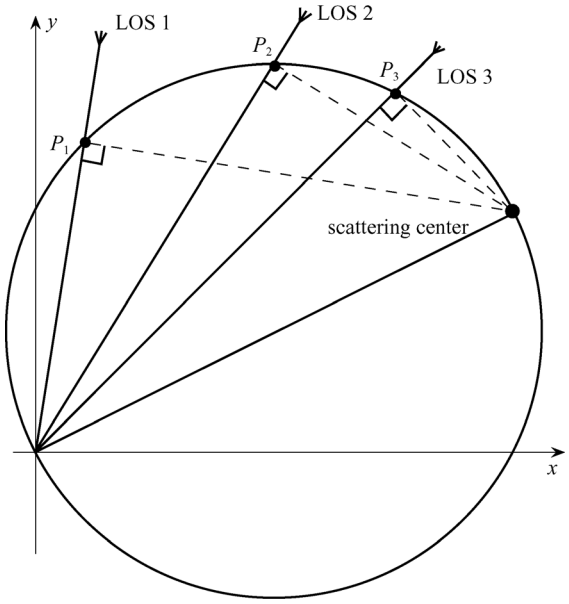

Fig. 2 Projection points of a fixed scattering center form a circle in the 2D case

The sphere placement of the projection points of a fixed scattering center is the base of our modeling method. The data points subordinating to one scattering center will naturally form a sphere (or a circle in the 2D case). Also, the far end of the diameter across zero indicates the space location

of this scattering center. The integrity of the sphere depends on the viewing angle extent of the corresponding scattering center and the scattering intensity of the data points on the sphere shows the variation in the scattering coefficient of the scattering center with the viewing angle.

Many scatterers such as tips, edges and trihedrals form fixed point scattering centers. However, there are scattering centers whose locations vary continuously to the change of the viewing angle. The backscattering of a smooth curved surface and the specular reflection of spheres and columns are cases in point. Their projection points will still form a continuous surface like a distorted sphere, and these scattering centers and their shape parameters can be extracted by deliberate modification of the algorithm. Besides these stable scattering centers, there are still many unstable scattering phenomena, such as the backscattering of a cavity, the backscattering caused by creeping or traveling waves, and the micro-Doppler phenomenon caused by kinetic parts on the target. How to merge these scatterers into the scattering center model is still a problem in the study of target characteristics [6,7]. Nevertheless, radar targets always contain many stable scattering centers and these stable centers are dominant target characteristics. Section 4 will demonstrate that the stable scattering center model can be used to reconstruct target signatures fairly well.

3 Algorithm description

Input: the wideband measurements at viewing angles that cover the concerned angular extent in a mesh style.

Output: the scattering center model that is valid in the concerned angular extent. It contains the position, type parameter and scattering coefficient matrix corresponding to the mesh grids for each scattering center.

Steps:

Step 1 1D scattering center parameter estimation at each viewing angle.

The following three factors should be especially considered in our application.

1) Retain sufficient dynamic range so that the stable scattering centers (e.g., the tip diffraction) will not be left out when there is strong specular reflection at some aspects.

2) High position estimation accuracy and good super-resolution ability: the super-resolution ability helps to reduce the interference between scattering centers when their 1D projective positions get close.

3) Stable and highly efficient algorithm: stability insures the consistent performance at different viewing angles and its efficiency insures the acceptable time consumption when the mesh grids amount is large.

We use the maximum a posteriori (MAP) probability criteria to select the 1D model order [9] and the structure total least norm (STLN) algorithm [10] to estimate other 1D scattering center parameters. Simulations show that the STLN algorithm outperforms other super-resolution algorithms such as ESPRIT and MUSIC in accuracy and stability, especially when dealing with measured or electromagnetic simulated data where model error exists.

Step 2 Position estimation of scattering centers.

Plot the projection points at the spatial location indicated by Eq. (3), the projection points at all the aspect angles constitute the OTSM. The spatial location of the stable scattering centers can be estimated by extracting the spheres in the OTSM map.

Sphere extraction is a typical problem in image processing. Several factors should be considered in particular according to the physical significance in our case:

1) A scattering center is visible in a limited angular extent, so the spheres in the OTSM map are always incomplete.

2) The projection points will not be on the sphere precisely because of the error in 1D parameter estimation.

3) The unstable scatterers of the target may produce noncontinuous projection points and these projection points will interfere with the sphere extraction as noisy data points.

4) The sliding scattering centers will form distorted spheres and the distortion depends on the shape of the scatterer.

The position estimation algorithm can be decomposed into the following substeps:

Substep 2-1 Extract the spheres in the OTSM map using Hough transform [11].

Substep 2-2 Associate the projection points [P_1, P_2,…, P_n] on the sphere (or within an error threshold of $\pm\,\Delta r/2$, where Δr is the Fourier resolution bin) with the corresponding scattering center according to the continuity of the amplitude/phase and the position of the projection points.

Substep 2-3 Substitute the parameters of the projection points (r_i, θ_i, γ_i), $i = 1,2,\ldots,I$ into Eq. (5a), and re-estimate the spatial location (x, y, z) of the scattering center.

$$r_i = x\cos\gamma_i\cos\theta_i + y\cos\gamma_i\sin\theta_i + z\sin\gamma_i, \quad i = 1,2,\ldots,I. \tag{5a}$$

Add other parameters in this equation and we can describe sliding scattering centers. For example, for a ball scatterer whose center is (x_o, y_o, z_o) and the radius is s, the equation can be modified as

$$r_i = x_o\cos\gamma_i\cos\theta_i + y_o\cos\gamma_i\sin\theta_i + z_o\sin\gamma_i + s, \quad i = 1,2,\ldots,I, \tag{5b}$$

where $s = 0$ is for the case of fixed scattering centers.

Substep 2-4 Repeat Substep 2-2 and Substep 2-3 until the convergency condition is satisfied. The convergency condition contains two parts:

a) The scattering center position estimated in this iteration is sufficiently close to that in the previous iteration.

b) There are enough effective projection points on the sphere corresponding to the scattering center in the OTSM map.

Step 3 Type parameter estimation.

There are two ways of estimating the type parameter: one is averaging or weighted averaging the type parameters of the scattering center at different angles, the other is determining the scattering mechanism of the scatterer according to its location. In fact, the type parameters have little effect on the total scattering field when the relative bandwidth is small. Therefore, the extrapolation performance of the model is not affected even if we set all the type parameters to be zeros.

Step 4 Complex amplitude estimation.

When the number of scattering centers and the 3D position and type parameter of each scattering center are set, Eq. (1) becomes a set of linear equations for a certain viewing angle (θ_i,γ_i). The scattering field at different frequencies $(f_1, f_2,\ldots, f_N)$ form the observation vector, the scattering coefficients $A_m(\theta_i,\gamma_i)$ form the estimation vector, and the remains form the $N \times M$ coefficient matrix. When $N > M$ (it must be satisfied), the coefficients of scattering centers at this aspect can be solved by the least squares method. Since projection points of different scattering centers may be close at some viewing angles, the coefficient matrix becomes singular in this case. So we do singular value decomposition (SVD) of the coefficient matrix, and the singular vectors with singular values smaller than $\sqrt{N}$ (this is the singular value for independent column vectors) are considered to compose the noise space. The estimates in the noise space should be obtained from the averaged original range profiles.

4 Simulation examples

Because of the data limitation, we only extract 2D models in the plane of elevation 0°.

4.1 Cone-sphere

The scattering data is predicted by the finite-difference time domain (FDTD) code and the target is ideally conductive. The computation parameters are: HH polarization, frequencies stepped from 9 to 11 GHz with 20 MHz interval, elevation angle 0°, azimuth angles stepped from 0° to 180° with 0.2° interval. The extracted model is shown in Fig. 3.

There are altogether five extracted scattering centers. The OTSM map visually reflects their scattering characteristics. The semi-sphere 3 is the strongest scatterer on this target and is very stable in both amplitude and location. The tip (scattering center 1) is a fixed scattering center and its scattering intensity is not strong especially when the line of sight departs from the normal line of the conical surface. The scattering centers on the edge (scattering center 2 and 5) are strong in scattering intensity but their locations fluctuate when the line of sight is near the conical surface. Scattering center 4 is very weak and is visible only when the line of sight is near the conical surface with severe location fluctuation. It may come from the traveling wave.

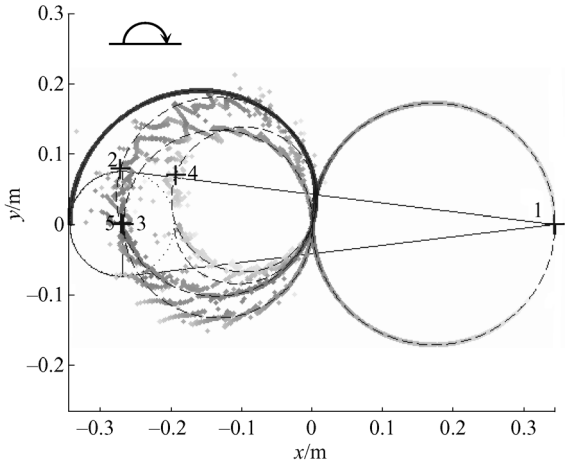

Overlaid by the extracted scattering centers ('+'), their corresponding circles (dashed line) and the contour of the target (bold lines). (the third center is sphere, dotted line is the estimated sphere, '+' is at the sphere's center)

Fig. 3 OTSM map of a cone-sphere

In addition, when the projection points of scatters 1 and 2 intersect, there are strong projection points in the OTSM map, and the backscattering mechanism turns from the diffraction of the tip and edge to the specular reflection of the cone side. Specular reflection usually comes from a smooth extended surface. This structure will produce edge diffraction on non-normal direction. Therefore, in the OTSM map, the specular projection points always appear at intersections of several projection circles. This phenomenon is also very obvious in the next example.

4.2 Boeing plane

The original data is predicted by a high frequency electromagnetic simulation code based on graphic electromagnetic computing (GRECO) [12]. The target is a full size Boeing 737 plane CAD model with the inlet duct and the cabinet covered. The target is ideally conductive. The frequency steps from 5 to 6 GHz with interval frequency 5 MHz; the elevation angle is 0° and the azimuth varies from 0° to 180° with angle interval 1°. The unambiguous range for cross imaging is only 1.7 m, thus we cannot get the target's 2D image directly from the original data. However, with the method in this paper, we can obtain the 2D scattering center model of the target and reconstruct the target's 2D image. To present the target's strong scattering structures under various polarizations, we com-

bine the OTSM maps at four polarizations (HH, VV, HV, VH) after normalization by their average energy respectively (since the scattering energy under cross-polarization is much smaller than that under co-polarization). The scattering centers extracted from the union OTSM map are shown in Fig. 4. The target's geometry model is shown in Fig. 5.

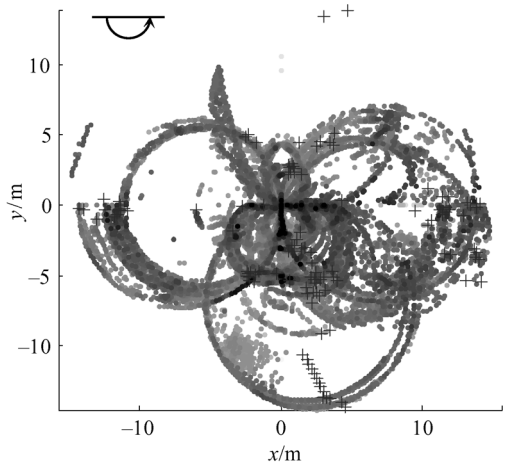

Fig. 4 OTSM map of B737 with four polarizations synthesized

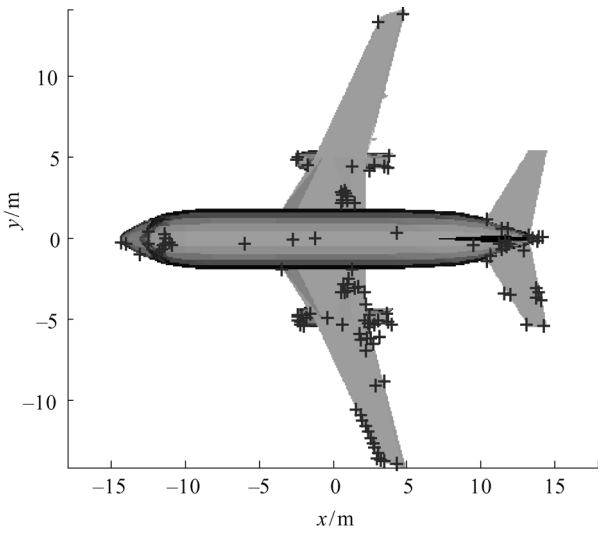

Fig. 5 Top view map of B737

In the OTSM map for complex targets, there are many noisy data points, non-complete projection circles and overlapped projection circles. Therefore, the parameters in Step 2 of the algorithm, such as the discrete cell of Hough transform, continuous condition, convergency condition and so forth, should be adjusted according to the target type, radar bandwidth, grid intensity, etc. For B737, there are 117 scattering centers extracted altogether as shown by '+' in Fig. 4. Compared with Fig. 5, it is easy to find that there are many edges and tips (such as three groups of wheels, the joint between the engine and airfoil) on the complex target and they produce many superimposed projection circles in the OTSM map. Therefore, for each structure a group of scattering centers with close locations is extracted and this greatly increases the number of the extracted scattering centers.

We can observe some scattering characteristics of the target from the OTSM map, such as the visible angular extent of the scattering center. For example, the wings' outer edge, the upright tail fin and the three groups of wheels under the body are visible at all viewing angles; the nose is visible within 0–90° while the side edge of the wing is only visible near the normal line. There are many dark points along the lines of $x = 0$ and $y = 0$. The reason is that the extended structures on the target are almost parallel to these axes, so there are many specular scatterers when the line of sight is perpendicular to the axes. Among these specular points, the backscattering of the fuselage is the strongest.

To verify the angle interpolation and frequency extrapolation performance, we compute other three groups of signature data of this plane model. Then we compare the data reconstructed by the scattering center model with the signatures computed by the high frequency software. Angle interpolation is realized by linear interpolation of the scattering coefficients on the space grid. Frequency extrapolation is realized according to Eq. (1).

1) Inverse synthetic aperture imaging

The parameters are as follows: the frequency steps from 5–5.5 GHz, the interval is 5 MHz with HH polarization, elevation angle is 0°, the azimuth varies from 0° to 5° with angle interval 0.05°. Thus, the resolution is 0.3 × 0.3 m. The original and reconstructed images are shown in Fig. 6. The amplitude and location of the peaks are almost consistent in these two subfigures. Comparing with Fig. 5, we find that the strong peaks are the nose, three groups of wheels and the front part of two engines.

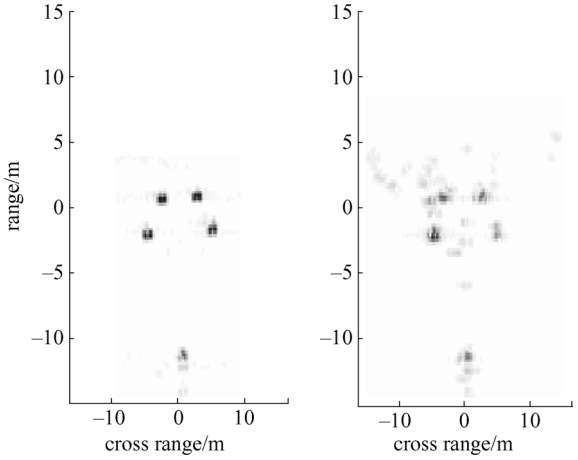

Fig. 6 Original image (left) versus rebuilt image

2) RCS fitting with angle interpolation

The frequency is 5 GHz with HH polarization, the elevation angle is 0°, the azimuth varies from 0° to 180° with angle interval 0.5°. The fitted result is shown in Fig. 7.

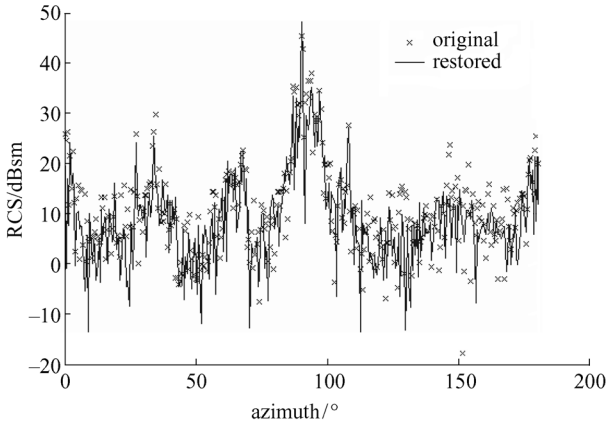

Fig. 7 Fitted RCS: interpolated angle results at C band

3) RCS fitting with frequency extrapolation.

The frequency is 9 GHz with HH polarization, the elevation angle is 0°, the azimuth varies from 0° to 180° with angle interval 1°. The fitted result is shown in Fig. 8.

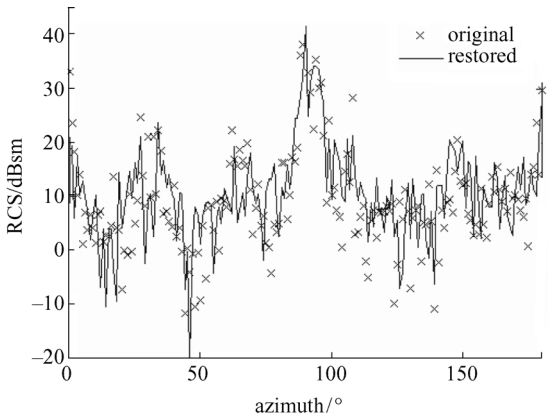

Fig. 8 Fitted RCS: extrapolated frequency results at X band

Since the scattering center model extracted by our method only contains stable scattering centers, the reconstructed RCS data are usually smaller than the original data, but they are identical in the changes of magnitude and variation.

5 Conclusions

We have proposed a method to extract the scattering center model of radar targets from wideband measurements covering a large angular extent by mesh grids. Since the continuity of the projective position and scattering coefficient of stable scattering centers is exploited, the density of the mesh grids can be much sparser than that used for radar imaging. This greatly cuts down the data amount needed for global scattering center model extraction. It is a practical modeling method that can be realized using measured or simulated data. Presented examples verify the effectiveness of the model in characteristic analysis and signature reconstruction.

Limited by the current data conditions, the presented example is only for 2D modeling in the plane of elevation angle 0°. The principle is also applicable for 3D modeling which is the goal of our future research. The difficulties to be solved includes: selecting proper spatial mesh grid, extracting spheres in the OTSM map, and visualizing the 3D OTSM, etc.

Now the data used to verify the model is produced by the same software used to produce the modeling data, and the original and fitted radar signatures (RCS, ISAR images) are only compared qualitatively. Further research will also aim at using reliable measured data to model complex targets and evaluate the model quantitatively.

Target recognition is an important application of the scattering center model. For example, it can be used to produce the high frequency radar images in real time at any viewing angle covered by the mesh grids, and this will greatly release the need for large memory to store the templates at different viewing angles [6]. Further research also includes designing other feature vectors based on the scattering center model to be used in target recognition applications.

Acknowledgements This work was supported by the National Basic Research Program of China (No. 51314).

References

1. Wang J, Nie Z P, Hu J, et al. Geometry construction rules of complex object's electromagnetic scattering analysis. Chinese Journal of Radio Science, 2003, 18 (1): 70–74 (in Chinese)
2. Xiang C W, Tong C M, Geng F Z, et al. Modeling method of decreased dimension for complex targets and its application in electromagnetic scattering analysis. Chinese Journal of Radio Science, 2005, 20(2): 189–192 (in Chinese)
3. Hughes E J, Leyland M. Using multiple genetic algorithms to generate radar point-scatterer models. IEEE Transactions on Evolutionary Computation, 2000, 4(2): 147–163
4. Bhalla R, Ling H. Three-dimensional scattering center extraction using the shooting and bouncing ray technique. IEEE Transactions on Antennas and Propagation, 1996, 44(11): 1445–1453
5. Kim K T, Kim H T. Two-dimensional scattering center extraction based on multiple elastic modules network. IEEE Transactions on Antennas and Propagation, 2003, 51(4): 848–861
6. Bhalla R, Moore J, Ling H. A global scattering center representation of complex targets using the shooting and bouncing ray technique. IEEE Transactions on Antennas and Propagation, 1997, 45(12): 1850–1856

7. Bhalla R, Ling H, Moore J, et al. 3D scattering center representation of complex targets using the shooting and bouncing ray technique: a review. IEEE Antennas and Propagation Magazine. 1998, 40(5): 30–39
8. Huang P K, et al. Radar Target's Signature. Beijing: China Astronautic Publishing House, 1993 (in Chinese)
9. Djuric P M. A model selection rule for sinusoids in white Gaussian noise. IEEE Transactions on Signal Processing, 1996, 44(7): 1744–1751
10. Huffel S Van, Park H, Rosen J B. Formulation and solution of structured total least norm problems for parameter estimation. IEEE Transactions on Signal Processing, 1996, 44(10): 2464–2474
11. Zheng N N. Computer Vision and Pattern Recognition. Beijing: National Defense Industry Press, 1998 (in Chinese)
12. Rius J M, Ferrando M, Jofre L. GRECO: Graphical electromagnetic computing for RCS prediction in real time. IEEE Antennas and Propagation Magazine, 1993, 35(2): 7–17